Multi-Frequency Radar Signal Processing for Moving Target Detection

Gong, Huaiyang ; Petrov, Nikita; Krasnov, Oleg; Yarovoy, Alexander

Publication date
2022

Document Version
Final published version

Published in
Proceedings of the 2022 23rd International Radar Symposium (IRS)

Multi-Frequency Radar Signal Processing for Moving Target Detection

Huaiyang Gong, Nikita Petrov, Oleg Krasnov, Alexander Yarovoy
Microwave Sensing, Signals and Systems (MS3)
Delft University of Technology
Delft, the Netherlands
ghyblanche@163.com, {N.Petrov, O.A.Krasnov, A.Yarovoy}@tudelft.nl

***Abstract*—This paper presents algorithms for joint signal processing of data from two radars located on the rooftop of TU Delft: PARSAX, operating in S-band, and MESEWI, operating in X-band [1]. In particular, the problem of data alignment in space (2D map) and time is addressed by observing moving targets of opportunity in the high-resolution mode. After the data alignment procedure, the detection algorithms for optimal fusing of dual-polarization and multi-frequency data are proposed. The detection results are considered the input for moving target (an auto) tracking and its signature extraction. The developed techniques were tested on the data records in experimental scenarios.**

***Index Terms*—Multi-frequency radar, data alignment, correlation**

I. Introduction

The radar lab of the Delft University of Technology has two middle-range radars, located on the rooftop of the EEMCW (Electrical Engineering, Mathematics and Computer Science) faculty building (Fig. 1). The radars are: PARSAX - an S-band polarimetric Doppler radar [2] and MESEWI - an X-band polarimetric Doppler scanning radar. The radar parameters important for this study are listed in Table I. As can be seen from Fig. 1, the radars are located in the vicinity of each other; therefore, we assume a mono-static configuration in what follows.

Until now, both radars have been used independently of each other for different applications: weather monitoring, moving targets detection and classification [3], [4], studying of the windmill [5], sea and vegetation clutter behavior, waveform analysis [6], [7] and others. Combining the data from both radars will open the opportunity to perform state-of-the-art research in multi-frequency dual-polarimetry data processing, important in several emerging applications.

The goal of this paper is to develop algorithms for data-based alignment of data from two radars in space and time. In particular, we focus on the data-based estimation of the relative position of the radars, which includes the estimation of the difference in cable lengths (PARSAX has relatively long cables – a few tens of meters – between the antenna and Tx / Rx chains, resulting in an additional range offset of the measurements) and subsecond estimation of the time difference between the radars during the measurements of moving targets of opportunity in the high range resolution (3 m) mode.

Fig. 1. Location of PARSAX and MESEWI radars on the roof of the EWI building

The remainder of this paper is organized as follows. In Sections II and III, we exploit targets of opportunity to perform spatial and temporal data alignment, respectively. In addition, in Section IV we combine the data from both radars to resolve the velocity ambiguities of moving targets and extract their range profiles. The results in all sections are supplemented by the results of real data processing. Finally, the conclusions are drawn in Section V.

TABLE I
Parameters of TU Delft polarimetric radars

Parameter	PARSAX	MESEWI
Carrier frequency, GHz	3.315	9.6
Antenna half-power beamwidth, deg	1.8 (Tx), 4.6 (Rx)	2.1 (both)
Bandwidth, MHz (max)	50 (100)	50 (300)
PRI, ms	1.02	0.61
Range cells	5100	1524
Signal separation for poalrimetry	Up / down chirps	TDMA

978-83-956020-5-4 ©2022 Warsaw University of Technology
IRS-2022, Gdańsk, Poland

II. Data alignment in space

A. Problem statement

Assume that MESEWI radar is located in the center of the Cartesian coordinate system, and PARSAX has a position displacement of δ_x and δ_y with the x and y axes aligned with the local latitude with the local meridian, respectively. Two radars observe a point-like target with Cartesian coordinates (x, y) at distances:

$$\begin{aligned} r^M &= \sqrt{x^2 + y^2} \\ r^P &= \sqrt{(x - \delta_x)^2 + (y - \delta_y)^2} + L_c, \end{aligned} \tag{1}$$

where r_P and r_M denote the range measurements to this target by PARSAX and MESEWI radars, respectively, and L_c stands for the cable length of PARSAX (in fact, it denotes the difference of cable lengths of both radars, but due to hardware realization, we assume that MESEWI has negligible cable length).

The objective is to estimate the unknown parameters: the cable length L_c of PARSAX and the position displacement between the two radars δ_x and δ_y. To solve this problem without referring to a set of fixed targets (the measurements of at least two targets are required in order to estimate three unknowns in (1)), we exploit the plan position indicator (PPI) images, obtained with both radars at the same elevation angles.

B. Spatial alignment procedure

The displacement of two images can be estimated by applying cross-correlation to them. It has been widely used for similar problems for decades, e.g. [8], [9]. The linear (for the selected coordinate system) shift between two images is estimated from the peak in the cross-correlation function, which efficiently can be computed using the fast Fourier transform (FFT). To exploit this property and perform the spatial alignment of the radar images, we estimate the unknown parameters in (1) in three steps:

1) Estimate the cable length: from the PPI images, represented in range-azimuth coordinates using cross-correlation. The length of the PARSAX radar's cable, denoted by L_c in (1) is estimated by:

$$\hat{L}_c = \underset{r}{\operatorname{argmax}}(\mathbf{P}^P(\theta, r) \star \mathbf{P}^M(\theta, r)), \tag{2}$$

where $\mathbf{P}^P(\theta, r)$ and $\mathbf{P}^M(\theta, r)$ are PPI images (the power values) of PARSAX and MESEWI, respectively, in range-azimuth coordinates; the operator $\star$ denotes digital correlation. Because the range and angular grids of the radars do not coincide with each other in a general setting, the measurements of PARSAX are interpolated to the range-angular grid of MESEWI prior to executing (2). For the presented below results, we use the bi-cubic interpolation (the results using the modified Akima cubic Hermite interpolation were similar). The parabolic approximation of the cross-correlation function near the maximum has also been used to minimize the impact of the grid [10]. The maximum search is applied in the range dimension only: the azimuth angles of both radars pointing are accurately known from the mechanical drives, which implies that the angular shift between the data sets is negligible (close to zero).

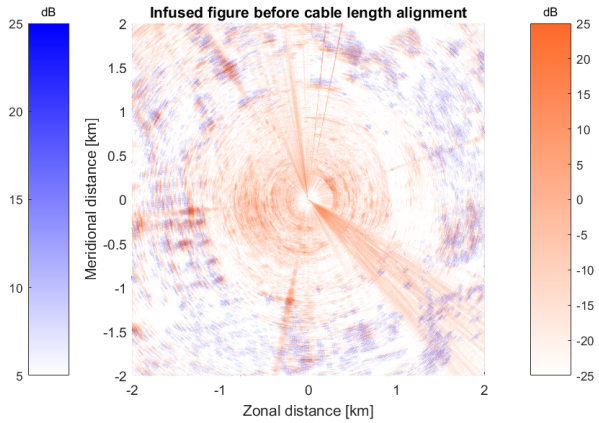

(a) Original PPI images

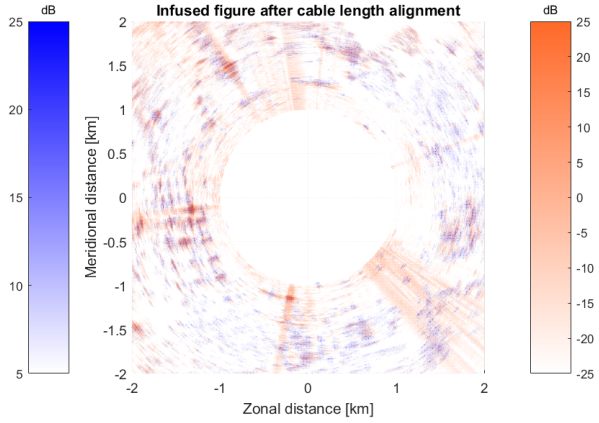

(b) After cable length compensation

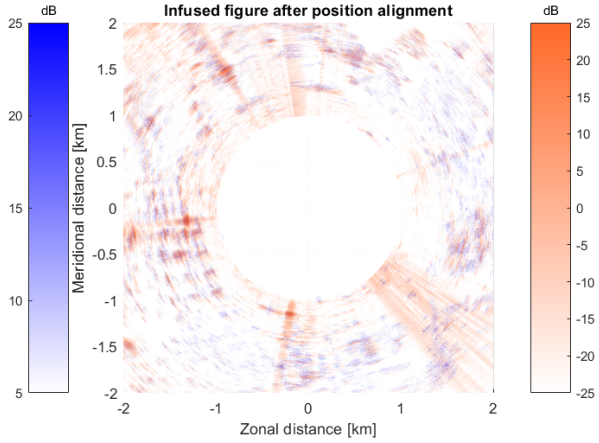

(c) After position alignment

Fig. 2. The infused PPI image of the two radars in Cartesian coordinates: blue - PARSAX data, red - MESEWI data.

2) Transform the data sets to Cartesian coordinates for each sample of both PPI images:

$$\mathbf{C}^R(x, y) = \boldsymbol{T}\{\mathbf{P}^R(r, \theta)\}, \tag{3}$$

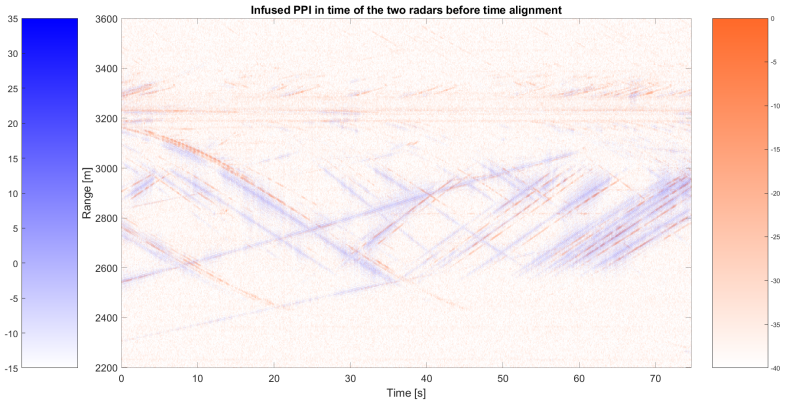

(a) Original measurments

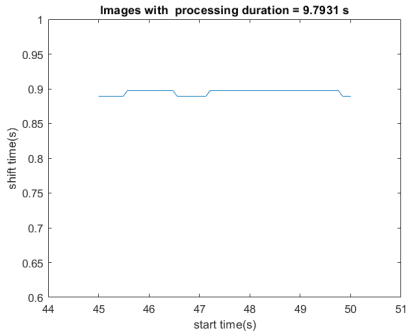

(b) Time difference

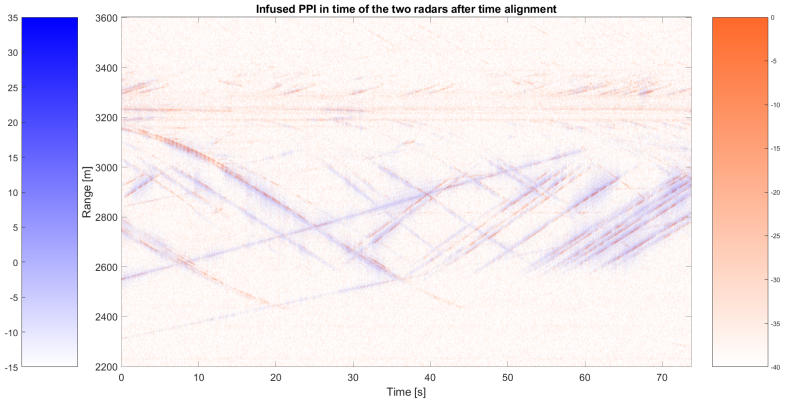

(c) Time-aligned measurments

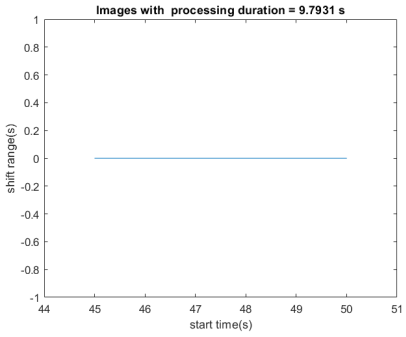

(d) Range difference

Fig. 3. Range/slow-time measurments of PARSAX and MESEWI before (a) and after (c) time aligment. Estimated time (b) and range (d) difference between the measurements as a function of time

where the operator $\boldsymbol{T}\{\cdot\} : (x, y) = (r\cos\theta, r\sin\theta)$ denotes the coordinate transformation and $R \in \{P, M\}$ indicates the considered radars. Here, we assume that the cable length has been corrected in the PARSAX data.

It should be noted that the assumption of collocated radars, which is crucial for the proposed solution, including estimation of cable length (2), is not correct at close ranges. For this reason before the cable length correction and further position alignment, we removed the measured data from ranges $r < R_0 = 1000$ m (see Figure 2). It reduces the effect of multipath propagation and reflections from objects on the roof (roof fence, radar antennas, and other equipment), which creates strong artifacts for data processing.

3) Radars relative position: can be estimated from the radar images in Cartesian coordinates by means of cross-correlation, similarly to the cable length estimation (2):

$$(\hat{\delta}_x, \hat{\delta}_y) = \underset{x,y}{\operatorname{argmax}}(\mathbf{C}^P(x, y) \star \mathbf{C}^M(x, y)). \tag{4}$$

To efficiently implement this procedure, we limit the data sets $\mathbf{C}^R(x, y), R \in \{P, M\}$ to the square inscribed in the circle, the radius of which is equal to the lower of two maximal measured ranges $r = \min\{r^P_{\max}, r^M_{\max}\}$. Moreover, we apply bi-cubic interpolation of the data sets $\mathbf{C}^R(x, y), R \in \{P, M\}$ to get the data samples on the linear uniform grids over x and y coordinates.

C. Application to the measured data set

The procedure described above has been applied to the measured PPI images of PARSAX and MESEWI radars. The results are presented in Fig. 2. The amplitudes of the reflected signals in the ranges from 0 to 1000m from the radar were replaced by 0 to avoid the influence of interference from the roof reflections.

The estimated cable length of PARSAX is equal to $\hat{L}_c = 36.83$ m and the relative position of the radars is equal to $(\hat{\delta}_x, \hat{\delta}_y) = (2.34, -9.13)$ m. These results agree well with the physical placement of the radars (see Fig. (1)) and the available data on the cables.

III. Data Alignment in Time

A. Problem statement

The header of every data block collected by both radars is labeled with a time stamps, updated every second (MESEWI

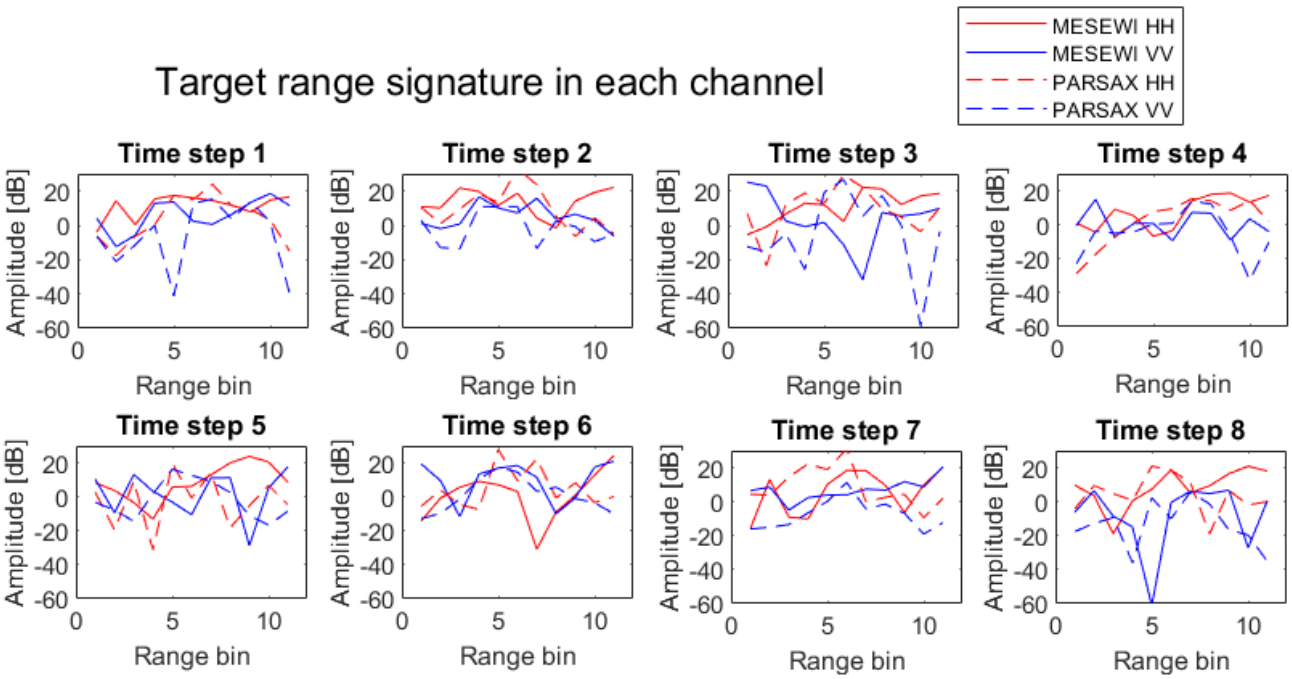

Fig. 4. Extracted range signature of an auto in each channel

uses time stamps from GPS; PARSAX uses the time from the Internet). For both radars, the data blocks contain 512 slow-time range profiles, measured with the PRI mentioned in Table I. We aim at observing the signatures of the moving target (cars on the highway) in a dual-frequency mode. Therefore, the time difference between radars δ_T up to one second is definitely not sufficient for proper alignment of moving target signatures: a car moving with the radial velocity of $v_0 = 30$ m/s would appear in the radar range-Doppler images at different ranges up to ten ($\delta_T v_0/\Delta_R \leq 10$) range cells. To deal with this issue, we develop a procedure to estimate the time difference between the radars from the measured data.

B. Time alignment procedure

For the time alignment, we consider that the measurements were taken with both radars at the fixed pointing angle and that a few moving targets of opportunity were observed. The data is pre-processed to compensate for displacement in the selected azimuth direction according to the radars' positions and cable length described above. A two-pulse canceller is applied to the data sets to reduce the impact of ground clutter. We also assume that the targets have relatively high SNR, such that they can be seen in the range/slow-time image. With this pre-processing, the time difference is estimated via cross-correlation:

$$(\hat{\delta}_t, \hat{\delta}_r) = \underset{t,r}{\operatorname{argmax}}(\mathbf{S}^P(t,r) \star \mathbf{S}^M(t,r)), \tag{5}$$

where $\mathbf{S}^R(t,r), R \in \{P, M\}$ denotes the slow-time/range image (power) of the radar. The search over the range dimension is applied to verify the correctness of the position alignment. Note that, due to the different PRF settings of the radars, interpolation is applied before digital correlation: MESEWI data, as the one collected with higher PRF, is interpolated to the PARSAX time grid.

C. Application to the measured data set

We apply the proposed procedure to the measurements of the N470 road (between Delft and Pijnacker), which has one line in every direction. We use the same radar settings as before, see Table I. Measurements before and after alignment are presented in Fig. 3, (a) and (c), respectively. It can be seen that the trajectories of some strong targets, present for a long interval in the scene are parallel before time alignment (Fig. 3, (a)) and they coincide well after applying the proposed technique (Fig. 3, (c)). For performing this alignment, we applied a sliding window of 9.8 s to the data set and got different results as a function of measurement time: the results in Fig. 3, (b, d) demonstrate the consistency of such time and range alignment over the presence of different targets in the scene.

IV. Velocity Ambiguity Resolution and Target Signature Extraction

A. Velocity ambiguity resolution

The setup of the radars implies that both of them observe the cars on the highway, may exceed half of the velocity ambiguity, and appear at false Doppler frequency. The velocity ambiguities of the radars are: $v_a^P = \lambda^P/(2T^P) = 44.4$ m/s and $v_a^M = \lambda^M/(2T^M) = 12.8$ m/s. The difference in denominators is due to the fact that full polarimetric measurements

are realized in PARSAX via up/down chirps for separation of signals with different polarizations, while MESEWI uses time division multiplexing (TDMA). Hereinafter, we use only co-polarized data channels. When using both radars for observing the same scene, velocity ambiguities can be resolved directly from the data, even if both radars operate at a single low PRF mode.

To combine the detection from both radars without velocity ambiguities, we applied the following rule:

$$R = (P_{HH} \wedge M_{HH}) \vee (P_{HH} \wedge M_{VV}) \vee (P_{VV} \wedge M_{HH}) \vee (P_{VV} \wedge M_{VV}), \quad (6)$$

where P_c and M_c denote the logical output of the CFAR detector on the PARSAX and MESEWI radars in the polarimetric channel c, respectively. The rule can be interpreted as: the target is declared detected if it is detected by both radars simultaneously in at least one polarimetric channel.

B. Target signature extraction

After the velocity ambiguities are resolved, we can estiate the appropriate target velocity and extract its range signature. Since the logic output of one target may cover several range/Doppler cells, we group the primitive detections using the K-means clustering algorithm [11]. The gravity center of the cluster (range and Doppler) is used as input to the Kalman filter to estimate the range trajectory of the target. Since the tragets do not move directly to the radial direction of the radars, it becomes possible to have their signature analisys from different aspect angles in dual frequency simultaneously. An example of the extracted car signature in the S and X bands is presented in Fig. II-C. The example demonstrates the variability of the range response of a car over time, frequency, and polarimetry. A proper combination of all these channels is foreseen to bring an improvement in the separation of the targets from clutter and their classification.

V. Conclusion

The paper presents a set of algorithms for joint multi-frequency dual-polarimetric data processing from two middle-range radars available at TU Delft: PARSAX and MESEWI. A procedure of spatial and temporal alignment of measured data is proposed. It allows resolving velocity ambiguities when both radars operate at a single low PRF mode and make possible the extraction of target signatures in dual-polarimetry at two frequency bands simultaneously. This preliminary study opens the possibility for future research being performed with these unique research facilities.

References

[1] "TU Delft, Microwave Sensing, Signals and Systems: RadarLab," http://radar.tudelft.nl/Facilities/radarlab.php.

[2] O. A. Krasnov, L. P. Ligthart, Z. Li, P. Lys, and F. van der Zwan, "The parsax-full polarimetric fmcw radar with dual-orthogonal signals," in *2008 European Radar Conference*. IEEE, 2008, pp. 84–87.

[3] N. Petrov and F. Le Chevalier, "Iterative adaptive approach for unambiguous wideband radar target detection," in *2015 European Radar Conference (EuRAD)*. IEEE, 2015, pp. 45–48.

[4] Y. Cai, O. Krasnov, and A. Yarovoy, "Radar recognition of multi-propeller drones using micro-doppler linear spectra," in *2019 16th European Radar Conference (EuRAD)*. IEEE, 2019, pp. 185–188.

[5] O. Krasnov and A. Yarovoy, "Polarimetric micro-doppler characterization of wind turbines," in *2016 10th European Conference on Antennas and Propagation (EuCAP)*. IEEE, 2016, pp. 1–5.

[6] Z. Wang, F. Tigrek, O. Krasnov, F. Van Der Zwan, P. Van Genderen, and A. Yarovoy, "Interleaved ofdm radar signals for simultaneous polarimetric measurements," *IEEE Transactions on Aerospace and Electronic Systems*, vol. 48, no. 3, pp. 2085–2099, 2012.

[7] U. Kumbul, N. Petrov, F. van der Zwan, C. S. Vaucher, and A. Yarovoy, "Experimental investigation of phase coded fmcw for sensing and communications," in *2021 15th European Conference on Antennas and Propagation (EuCAP)*. IEEE, 2021, pp. 1–5.

[8] P. E. Anuta, "Spatial registration of multispectral and multitemporal digital imagery using fast fourier transform techniques," *IEEE Transactions on Geoscience Electronics*, vol. 8, no. 4, pp. 353–368, 1970.

[9] T. J. Keating, P. Wolf, and F. Scarpace, "An improved method of digital image correlation," *Photogrammetric Engineering and Remote Sensing*, vol. 41, no. 8, pp. 993–1002, 1975.

[10] E. Jacobsen and P. Kootsookos, "Fast, accurate frequency estimators [dsp tips & tricks]," *IEEE Signal Processing Magazine*, vol. 24, no. 3, pp. 123–125, 2007.

[11] D. Arthur and S. Vassilvitskii, "k-means++: The advantages of careful seeding," Stanford, Tech. Rep., 2006.